Food Hydrocolloids for Health 2 (2022) 100097

Contents lists available at ScienceDirect

Food Hydrocolloids for Health

journal homepage: www.elsevier.com/locate/fhfh

Fine-tuning of functional and structural properties of Ca(II)-alginate beads containing artichoke waste extracts

Ignacio Zazzali[a,b], Gabriela Jaramillo[c], Julieta Gabilondo[a,d], Luana Peixoto Mallmann[e], Eliseu Rodrigues[e], Mercedes Perullini[f,g], Patricio R. Santagapita[a,b,*]

[a] Universidad de Buenos Aires. Facultad de Ciencias Exactas y Naturales. Departamentos de Química Orgánica y de Industrias. Buenos Aires, Argentina
[b] CONICET-Universidad de Buenos Aires. Centro de Investigaciones de Hidratos de Carbono (CIHIDECAR). Buenos Aires, Argentina
[c] CONICET-Universidad de Buenos Aires. Instituto de Tecnología de Alimentos y Procesos Químicos (ITAPROQ). Buenos Aires, Argentina
[d] Instituto Nacional de Tecnología Agropecuaria (INTA) Estación experimental agropecuaria (EEA). San Pedro. Ruta 9 km 170. Buenos Aires. Argentina
[e] Instituto de Ciência e Tecnologia de Alimentos, Universidade Federal do Rio Grande do Sul, Av. Bento Gonçalves 9500, Porto Alegre 91501-970, Brazil
[f] Universidad de Buenos Aires. Facultad de Ciencias Exactas y Naturales. Departamento de Química Inorgánica, Analítica y Química Física. Buenos Aires, Argentina
[g] CONICET-Universidad de Buenos Aires. Instituto de Química Física de los Materiales, Medio Ambiente y Energía (INQUIMAE). Buenos Aires, Argentina

ARTICLE INFO

Keywords:
Encapsulation
Microstructure
Biopolymers
Waste
Bioactive compounds
RSM

ABSTRACT

Artichoke harvest waste is rich in phenolic compounds, which we retrieved with green extractions to exploit this otherwise undervalued material. Here, to protect these labile compounds, we encapsulated the extract into Ca(II)-alginate beads and optimized their physico-chemical and structural properties via response surface methodology. Moreover, we corroborated the carryover of predominant phenolic compounds from waste to bead via high-performance liquid chromatography coupled with diode-array detection and mass spectrometry (HPLC-DAD-MS). We found that maximum bioactive capacity is obtained at higher concentrations of alginate precursor and lower gel consolidation times and that strength, size, and roundness of the beads were influenced mainly by the alginate precursor concentration. Additionally, through small angle X-ray scattering we revealed a deep relationship between synthesis conditions and the microstructure of the gel, related to the crosslinking degree and ramification of the final arrangement, which in turn impacts its strength. We validated the model by running an optimal point of 2 min of gelling time and 2.25 % of alginate and obtaining satisfactory experimental errors for the parameters analyzed. This holistic approach enables modulation and bottom-up tuning of the structure of beads for advanced delivery applications.

1. Introduction

United Nations Sustainable Development Goals (SDG) call society for action to guarantee the protection of the planet and the lives of people. Specifically, SDG #2 and #3 set goals of zero hunger and good health and well-being, respectively. Approximately one-third of all the food produced for human consumption is wasted every year regardless of the level of development of countries. Moreover, in developing countries, 40% of those losses occur at post-harvest and processing levels (FAO, 2019). In this regard, researchers and manufacturers should make efforts to bolster the supply chain from the early stages and intend to exploit every bit of what is produced. Furthermore, to contribute to a more holistic approach to human health, efforts should be made to develop and promote functional foods with an aim not only in the enhancement of nutritional values but also in bioactive properties.

Bioactive compounds are substances that exhibit biological activity related to their ability to modulate metabolic processes (Santos et al., 2019; Serrano et al., 2016) and can help prevent diseases such as coronary heart disease, cancer, gastrointestinal and neurodegenerative conditions (Astley & Finglas, 2016). They include carotenoids, phytosterols, glucosinolates, vitamins (Santos et al., 2019) and phenolic compounds (Tungmunnithum et al., 2018; Zazzali et al., 2021). However, these compounds have been reported to present low stability and poor absorption in the digestive tract and can be susceptible to environmental conditions such as light, temperature, pH, oxygen and enzymes (Madalena et al., 2019). For these reasons, encapsulation methods are studied to preserve their integrity and to tailor and enhance their release behavior. Alginate, a natural anionic and hydrophilic linear biopolymer, is commonly used to encapsulate labile bioactive compounds (Aguirre Calvo et al., 2018). In presence of divalent cations such as Ca^{2+}, crosslinking occurs

* Corresponding author.
E-mail address: patricio.santagapita@qo.fcen.uba.ar (P.R. Santagapita).

https://doi.org/10.1016/j.fhfh.2022.100097
Received 2 August 2022; Received in revised form 21 September 2022; Accepted 3 October 2022

(Stokke et al., 2000) leading to the formation of an hydrogel widely used for immobilizing bio-entities, mostly in the form of beads (He et al., 2016; Narayanan et al., 2012; Perullini et al., 2014).

While encapsulation efficiency is a paramount criterion to establish and optimize an encapsulation procedure, variations in the method may also induce changes in the physical properties of the beads such as their size, appearance, and mechanical strength. It is well known that appearance is a critical aspect in the appeal of food products and ingredients, as is the shape which can also alter how we perceive the food both visually and gustatorily (Spence & Ngo, 2012). Beads should also be able to withstand shear stress and not break during industrial processing for their incorporation into other products such as functional foods. Some studies have focused on the optimization of synthesis parameters in Ca(II)-alginate encapsulation by Response Surface Methodology (RSM) analyzing the response of a variety of physical and chemical properties (Jeong et al., 2020); however, little work has been done on the analysis of the variations in the fine internal structure of the gel matrix.

Several key properties of the material (i.e., the release rate of the encapsulated compounds, beads strength, etc.) are highly dependent on the supramolecular alginate network (Aguirre Calvo et al., 2020, Jeong et al., 2020). The study of the microstructure-function relationships in alginate-based capsules requires a microstructure characterization technique suitable for the elucidation of the alginate network parameters in native hydrogels (i.e., without drying or other pretreatments that could affect their microstructure and texture) (Agulhon et al., 2012). Small angle X-ray scattering (SAXS) is a powerful method for the analysis of hydrogels and has been employed previously to elucidate and assess microstructural changes in alginate-based beads for variations in the encapsulation procedure (Traffano-Schiffo et al., 2018; Zazzali et al., 2019). This technique is based on the correlation between the fluctuations in the electron density of the hydrogel lattice and its X-ray scattering pattern and allows inferring information about the structure of the pristine hydrogel on a scale of 1 to 100 nm (Traffano-Schiffo et al., 2018).

Globe artichoke (*Cynara scolymus L.*), an herbaceous plant belonging to the *Asteraceae* family, is very rich in phenolic compounds, mainly caffeoylquinic and dicaffeoylquinic acids (Lattanzio et al., 2009; Zazzali et al., 2021) as well as the prebiotic inulin, minerals, and fibers. In a previous study (Zazzali et al., 2021) we characterized every part of the artichoke agricultural waste (bracts, stem and leaves) of three varieties (Sampedrino, Gallego, Gringo) produced in the INTA experimental station in San Pedro, Argentina, and we optimized the extraction of their bioactive compounds with a green and cheap water-based extraction method. Based on that research and in an effort to conserve the bioactive compounds and introduce them in a medium suitable for functional foods and delivery applications, this work aimed to optimize its encapsulation in Ca(II)-alginate beads via a response surface methodology. This method allowed for the study of the influence of some synthesis variables on the macro- and micro-structure of the gel matrix and the obtainment of desirable physicochemical attributes. Finally, an HPLC-MS analysis was employed to identify the phenolic compounds present in the artichoke fresh sample and their carry-over to the aqueous extract and the Ca(II)-alginate beads.

2. Materials and methods

2.1. Materials

Sodium alginate: Algogel 5540 (Cargill S.A San Isidro, Buenos Aires, Argentina), MW of 1.97 (± 0.06) 10^5 g mol^{-1} and mannuronate/guluronate ratio of 0.6; $CaCl_2.2H_2O$ (98 %, Cicarelli S.A., Argentina).

HPLC grade acetonitrile and methanol were purchased from J. T. Baker (Phillipsburg, NJ). Formic acid was purchased from Merck (Darmstadt, Germany). Methanol (P.A.) was purchased from Neon Comercial (São Paulo, Brazil). Ultrapure water (Milli-Q) was generated by the Millipore System (Molsheim, FR). The samples and solvents were filtered through cellulose acetate (aqueous solutions) or polytetrafluoroethylene (organic solutions) membranes of 0.22 μm.

2.2. Artichoke sample collection and post-harvest treatment

Artichokes of the Sampedrino variety were cultivated in the INTA establishment in Buenos Aires, Argentina, in 2018. They were collected in September 2018 throughout various harvests. Once collected, leaves (L), bracts (B) and stems (S) were separated. They were washed and a portion of the samples was blanched for 5 or 10 minutes with steam. Afterward, all samples were stored in an ultra-freezer (Thermo Scientific, model forma 900 series, USA) at -70°C until analysis.

2.3. Extraction procedure

One gram of sample was thawed at 40°C in a sand bath for 30 minutes. Then, the sample was finely cut with a knife, crushed with pestle and mortar and 10 mL of double distilled water at 25°C were added. Extraction was carried out in the dark for 1 hour under constant magnetic stirring as optimized in our previous work (Zazzali et al., 2021). After the extraction, samples were filtered, diluted to 50 mL with double distilled water, centrifuged for 15 minutes at 11200 g and collected for later encapsulation.

2.4. Beads preparation

Sodium alginate was dissolved in 4.00 mL aliquots of the artichoke selected aqueous extract (pH = 5.5) under constant stirring to obtain solutions in concentrations ranging from 1.25 % to 2.25 % (w/v). Calcium chloride solution (2.50 % (w/v) was prepared under constant stirring in a 1.0 M acetate buffer pH 5.5. Beads systems for the RSM were prepared by ionotropic gelation using a dropping method (Zazzalli et al., 2019). Succinctly, 4 mL of the alginate solutions were dripped using a peristaltic pump model BT50-1J JY10 (Baoding Longer Precision Pump Co., Ltd., China) with a 0.40 mm extrusion tip connected to a silicone tube of 1 mm internal diameter at 6.0 (± 0.1) cm over 40 mL of $CaCl_2$ solution under constant stirring. The complete extrusion of the alginate solution took approximately 2 minutes. Once the last bead was generated, they were maintained in the gelling bath between 2 and 6 min according to the RSM points. Subsequently, beads were collected and washed out 3 times with distilled water and stored without residual solution, as previously optimized (Zazzali et al., 2019). A total of 9 systems containing encapsulated phenolic compounds corresponding to the RSM points and 1 additional control (the central point of the RSM without phenolic compounds) were prepared. Systems were kept at 4 (±1) ° C until use.

2.5. Total phenolic content (TPC)

An adaptation of the procedure proposed by Singleton & Lamuela-Raventós (1999) was followed for the determination of the total phenolic content of extracts. Briefly, 3 beads of each system were dissolved in 50 μL of 20% (w/v) sodium citrate solution under agitation in a vortex for 40 min. Samples were then mixed with 800 μL of double-distilled water, 125 μL of sodium carbonate solution (20 % (w/w)) and 125 μL of Folin-Ciocalteau reagent (Biopack, Zárate, Buenos Aires, Argentina). After reaction at 40°C in the dark for 30 minutes, samples were centrifuged at 11200 g for 5 min and absorbance was measured at 765 nm. Gallic acid (GA) standard was used to make a calibration curve. TPC was calculated as mg gallic acid equivalents mL^{-1} and results were expressed as loading efficiency of total phenolic content (TPC L.E) as in the following equation, where TPC_{beads} is the total phenolic content of liquefied alginate beads normalized by volume and $TPC_{extract}$ is the total phenolic content of the extract:

$$TPC\ L.E\ (\%) = \frac{TPC_{beads}}{TPC_{extract}} * 100$$

2.6. $ABTS^{\bullet+}$ radical cation scavenging ability (ABTS SA)

A technique described by Re et al. in 1999 was used to determine the ability of samples to scavenge the radical $ABTS^{\bullet+}$ (2,2-azinobis-(3-ethylbenzothiazoline-6-sulfonate)). ABTS (7 mM) was left to react 16 hours in the dark with potassium persulfate (2.45 mM). After this period, the solution was diluted with 0.01 M phosphate buffer at pH 7.4 until an absorbance 0.7 at 734 nm was obtained. Three beads of each system were dissolved in 100 μL of sodium citrate solution (10% (w/v)) for 40 min under agitation in a vortex. An aliquot of 1.9 mL of the $ABTS^{\bullet+}$ reagent was then added to each sample and this mixture was incubated at 25°C for 30 min in the dark. Afterward, the absorbance of the reaction mixture was measured at 734 nm and the percentage of color inhibition was confronted against gallic acid calibration curve. Scavenging ability (SA) for the $ABTS^{\bullet+}$ free radical was calculated as mg gallic acid equivalents mL^{-1} and expressed as residual ABTS SA (RSA) as in the following equation, where SA_{beads} is the scavenging ability of liquefied alginate beads normalized by volume and $SA_{extract}$ is the scavenging ability of the extract:

$$RSA\ (\%) = \frac{SA_{beads}}{SA_{extract}} * 100$$

2.7. Ferric reducing antioxidant power (FRAP)

The ferric reducing antioxidant power of the samples was obtained according to the method explained by Benzie & Strain in 1996. To form the FRAP reagent, 25 mL of 0.3 M acetate buffer at pH 3.6, 2.5 mL of aqueous 20 mM iron chloride (III) solution and 2.5 mL of 10 mM 2,4,6-Tris(2-pyridyl)-s-triazine (TPTZ) in 40 mM HCl were mixed. Shortly, 2 beads of each system were dropped in 840 μL of newly prepared FRAP reagent and after 30 min of incubation in the dark at 25°C, absorbance was read at 595 nm. The calibration curve was constructed in the same fashion using 2 empty beads dropped into standard solutions of different concentrations of gallic acid. Ferric reducing antioxidant power (FRAP) was calculated as mg gallic acid equivalents mL^{-1} and expressed as residual FRAP (RFRAP) as in the following equation, where $FRAP_{beads}$ is the ferric reducing antioxidant power of liquefied alginate beads normalized by volume and $FRAP_{extract}$ is the ferric reducing antioxidant power of the extract:

$$RFRAP\ (\%) = \frac{FRAP_{beads}}{FRAP_{extract}} * 100$$

2.8. Macroscopic characterization

Feret's diameter and roundness were analyzed with the free license software ImageJ by executing the "analyze particle" command as described by Zazzali et al. (2019). Roundness represents how far the shape is from sphericity, by relating the area to the major axis of the beads. A digital camera (Canon digital camera, 3.2 Mpix PowerShotA70; Canon Inc., Malaysia; with zoom fixed at 3x) coupled with a binocular microscope (Unitron MS, Unitron Inc., New York, USA, magnification at 7x) was used to take pictures of at least 30 beads for each point of the RSM.

2.9. Microstructural analysis

Traffano-Schiffo and co-workers (2018) modeled the structure of the Ca(II)-alginate matrices as a mass fractal system of interconnected alginate rods characterized by SAXS. Three parameters were obtained from the analysis: the fractal dimension at low q values (< ~0.28 nm^{-1}), denoted as α_1, describing the connectivity between rods in the network at a large scale (>10 nm); the fractal dimension at intermediate q values (α_2) describing the degree of compactness within the rods and the density of alginate dimers (α_3) at high q values (> ~1.9 nm^{-1}). SAXS experiments were carried out at the LNLS SAXS1 beamline in Campinas, Brazil, working at $\lambda = 0.1488$ nm and wave vector (q) was selected in the range 0.142 nm^{-1} < q < 5.040 nm^{-1}.

2.10. Beads strength

A compression assay was performed to determine the maximum force that was applied to each of the Ca(II)-alginate beads. A Texture Analyzer (model 3345, Instron, USA) was employed with a 3.0 mm diameter probe by applying compression of 25 % to a single bead, using a test speed of 0.1 mm/minute at room temperature (20 ± 1°C), with a loading charge of 50 N. Beads were placed centrally, under the probe and 10 individual samples were analyzed for each system.

2.11. Phenolic compounds analysis by HPLC-DAD-MS

The phenolic compounds were exhaustively extracted from freeze-dried samples (0.50 g) using 5 mL of a mixture of methanol:water (8:2, v/v, acidified with 0.35% formic acid) and vortexing for 3 minutes. The extract was centrifuged at 3000 g for 5 minutes (4°C) and the supernatant was transferred to a flat bottom flask. This procedure was repeated until exhaustive extraction of the compounds (8 times). All extracts were combined and concentrated in a rotary evaporator to remove methanol (around 8 mL) before the LC-DAD-ESI-MS/MS analysis. Samples were analyzed in a Shimadzu (Kyoto, Japan) HPLC apparatus equipped with two LC-20AD pumps, a DGU-20A online degasser, a SIL20AHT automatic injector, a CTO-20A oven connected in a series to a DAD detector (SPD-M20A) and a mass spectrometer with a Quadrupole-Time-Of-Flight (QTOF) analyzer and an electrospray ionization source (ESI) (Bruker Daltonics, micrOTOF-Q III model, Bremen, Germany). The ESI source was operated in negative mode with conditions previously described by Rodrigues et al., (2013). The separation was carried out with a Phenomex C18 (250 mm x 4.6 mm) column with 4 μm packing. Solvents were classified as A (water acidified with 0.1% formic acid) and B (acetonitrile acidified with 0.1% formic acid). The samples were eluted according to the following binary gradient: 1% B as initial condition, 50% B from 1 to 50 min, 99% B from 52 to 57 min and 1% B from 60 to 67 min. The flow rate was 0.7 mL min^{-1}.

2.12. Response surface methodology and statistical analysis

The RSM used for the optimization of the encapsulation process was devised as a hexagon design with 9 points on the Design-Expert 11 software (Stat-Ease Inc., Minnesota, USA), as shown in Fig. S1 of the Supplementary File. The central point was repeated three times. The response of relevant factors for industrial applications and performance (TPC L.E, RSA, RFRAP, strength, roundness, and size of beads) as well as microstructural parameters (α_1, α_2, and α_3) on two independent synthesis factors (alginate concentration and gel consolidation time) was studied using three levels for the gel consolidation time (2 - 6 min) and five levels for alginate concentration (1.25 - 2.25 % w/v).

All measurements were analyzed by one-way ANOVA with Tukey's post-test by using Prism 6.01 (GraphPad Software Inc., San Diego, CA, USA) to assess the significant difference between mean values for each point in the RSM.

3. Results and discussion

3.1. Extraction of phenolic compounds

In a previous work (Zazzali et al., 2021) we characterized and quantified the phenolic content and biological properties of agricultural waste (stems, leaves and outer bracts) of three varieties of artichokes (Sampedrino, Gallego and Gringo) cultivated during 2017. We found that the stems of all varieties exhibited the highest quantities of phenolic compounds as well as antioxidant capabilities and Sampedrino was the most convenient variety to be further studied and exploited, both in terms of crop yield and phenolic compounds content. In this work, we analyzed samples of all the wastes of the Sampedrino variety cultivated during 2018 and found that stems showed the highest values of

Table 1
Regression coefficient table for the model of each response analyzed via RSM. Bold numbers indicate statistical significance in each model ($p<0.05$). The corresponding ANOVAs for each model are shown in Tables S1-S9.

	Intercept	Alginate concentration (% w/v)	Gel consolidation time (min)	Alginate concentration (% w/v) * Gel consolidation time (min)	Alginate concentration^2 (% w/v)	Gel consolidation time^2 (min)
TPC L.E (%)	30.53	**5.31**	**-3.66**			
p-values		**0.0011**	**0.0031**			
RSA (%)	15.68	**3.88**	**-3.7**			
p-values		**0.0066**	**0.0044**			
RFRAP (%)	22.94	0.33	**-1.7**			
p-values		0.51	**0.0089**			
Roundness	0.93	**0.03**	0.0022			
p-values		**0.0007**	0.52			
Feret's diameter (mm)	2.70	**0.12**	-0.013			
p-values		**0.0056**	0.52			
Alpha 1	1.49	-0.004	**-0.017**			
p-values		0.13	**0.0076**			
Alpha 2	3.53	**0.056**	**-0.046**			
p-values		**0.038**	**0.024**			
Alpha 3	1.24	**0.1**	-0.025	**-0.16**		
p-values		**0.0081**	0.29	**0.013**		
Strength (gf)	14.43	**0.4256**	**0.5525**		**0.1328**	**0.3123**
p-values		**0.0001**	**0.0001**		**0.0325**	**0.0005**

TPC, ABTS SA and FRAP confirming them as the major phenolic source among the waste (Fig. S2 of Supplementary File). We also implemented a post-harvest blanch procedure on the Sampedrino stem samples that further improved the TPC, ABTS SA and FRAP values of the samples, both for the 5 minutes and the 10 minutes procedure, as shown in Fig. S3.

3.2. Optimization of phenolic compounds encapsulation by RSM

The green extraction procedure was carried out on the Sampedrino stems with 5 minutes of blanching to obtain an aqueous extract. The TPC of the extract was 0.78 ± 0.03 mg_{GA}/mL, ABTS SA 0.22 ± 0.01 mg_{GA}/mL and FRAP 0.21 ± 0.01 mg_{GA}/mL. Subsequently, this extract was encapsulated in nine different Ca(II)-alginate bead systems following the conditions indicated by the RSM design. This form of encapsulation provides the phenolic compounds, otherwise free in solution, a vehiculization medium suitable for delivery applications and protects them from degradation during storage and human digestion (Aguirre Calvo et al., 2020).

In this work, we focused on the optimization of two fundamental and easily adjustable parameters of the dripping encapsulation process: the concentration of the alginate precursor solution and the gel consolidation time. Models proposed for the analyzed responses ranged from linear to 2FI, as can be deduced from Table 1. Statistical significance was achieved ($p < 0.05$ for the model) in all cases as well as a non-significant lack of fit, which indicates suitable modeling, as reported for each ANOVA in Tables S1-S9 of the Supplementary File. A difference of less than ~ 0.2 was also achieved between the predicted R^2 and adjusted R^2 in each model, and low CV% values. As can be seen in Table 1 and Fig. 1, the models obtained for the response of TPC, ABTS SA and FRAP were all linear functions of the synthesis parameters. While TPC and ABTS SA were influenced both by gel consolidation time and alginate concentration ($p < 0.05$ for both factors, Table 1), FRAP was only influenced by gel consolidation time ($p < 0.05$). Although in previous studies we have found a direct correlation between the TPC, ABTS SA and FRAP of our aqueous extracts obtained from artichokes, the FRAP is influenced by non-phenolic bioactive compounds as well, which in a Ca(II)-alginate environment could present different interactions than phenolic compounds with the gel matrix, thus not presenting analogous correlation when encapsulated. Furthermore, it should be noted that, due to interferences between the FRAP reagents and the sodium citrate used for beads dissolution, the methodology used for this assay relies on the diffusion of the bioactive compounds into the sample solution rather than a complete dissolution of the beads. Therefore, in this assay, most compounds responsible for the FRAP response are those able to diffuse through the beads thus decreasing the relative importance of intermolecular interactions in the gel matrix of those that are not capable of diffusing.

On the one hand, it was expected that a higher gel consolidation time would lead to less bioactive compounds encapsulated since more diffusion into the gelation bath would be permitted. Aguirre Calvo and co-workers (2018) found similar results even getting to the point of coloration of the gelling bath due to diffusion of pigment if beads were allowed to stay in it for enough time. On the other hand, higher concentrations of alginate, especially at elevated consolidation times, lead to bigger and more compact rod-like microstructures (Posbeyikian et al., 2021) which could enhance the interactions between the gel matrix and the encapsulated bioactive compounds. This phenomenon is upheld by the increase in the obtained microstructural parameters α_1, α_2, and α_3 as will be further discussed.

3.3. Structural modifications produced by changing RSM variables

As shown in Fig. 2-a and Table 1, the strength of the beads formulated in the RSM experiment showed a strong positive correlation with the gel consolidation time. As the droplet of alginate solution comes into contact with the gelling bath containing Ca^{2+} ions, gelation on the surface begins to occur and a spherical shape is developed to reduce the surface tension of the system (King, 1983). In consequence, the incipient network of Ca(II)-alginate forms and rearranges in the periphery of the initial droplet volume and free Ca^{2+} ions in solution diffuse through this incipient gel front into the interior of the bead leading to the gelification of the entire bead in a concentric manner generating a highly inhomogeneous microstructure (Sonego et al., 2016). Posbeyikian et al. showed in 2021 that it took 11 minutes for the complete gelification of a Ca(II)-alginate bead under very similar conditions to the present work. Consequently, it is plausible that, in the gel consolidation times studied here, beads had not reached a complete gelification leading to substantial differences in the proportion of liquid core to gel network for each RSM point. Regardless of the short times studied in this work, gels allowed to consolidate for longer times were stronger, possibly due to a higher availability of Ca^{2+} cations leading to a higher degree of crosslinked chains as also showed by Posbeyikian et al. (2021).

The concentration of the alginate solution was also found to be directly proportional to the strength of the beads (Table 1) possibly related to a more compact and consolidated internal structure as

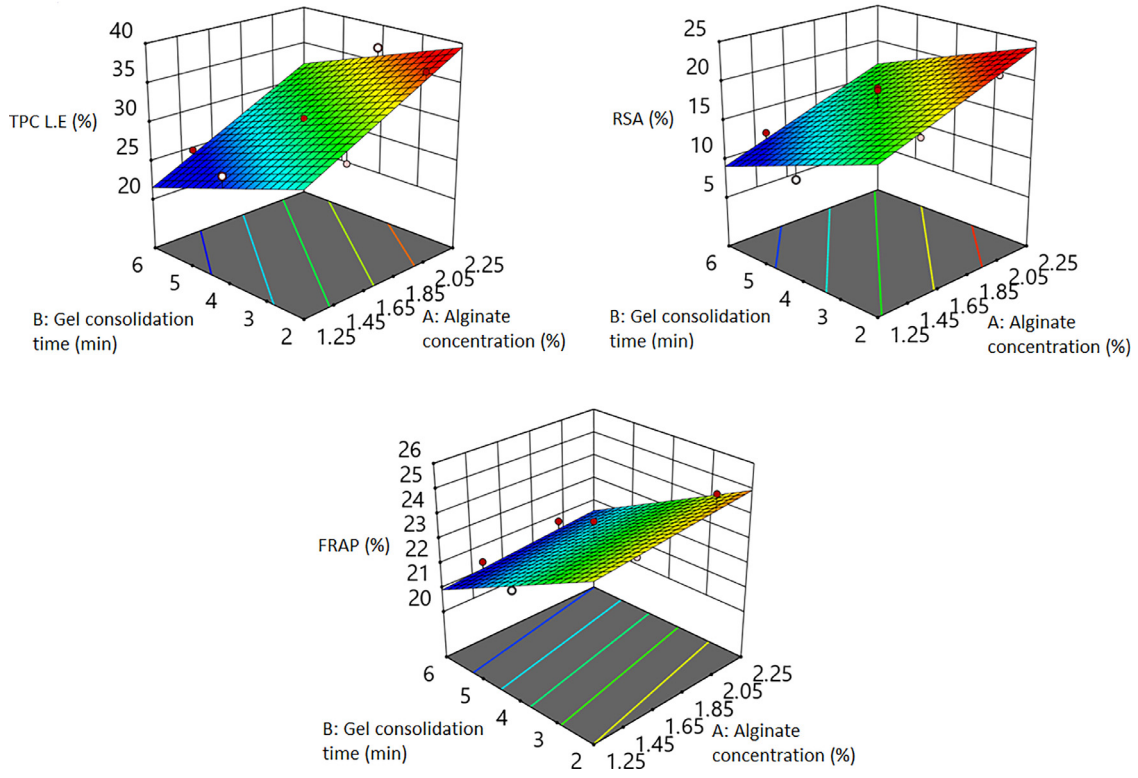

Fig. 1. RSM 3d surface for biological activity: A) TPC L.E, B) RSA and C) RFRAP, expressed in percentage (%) for each point in the RSM.

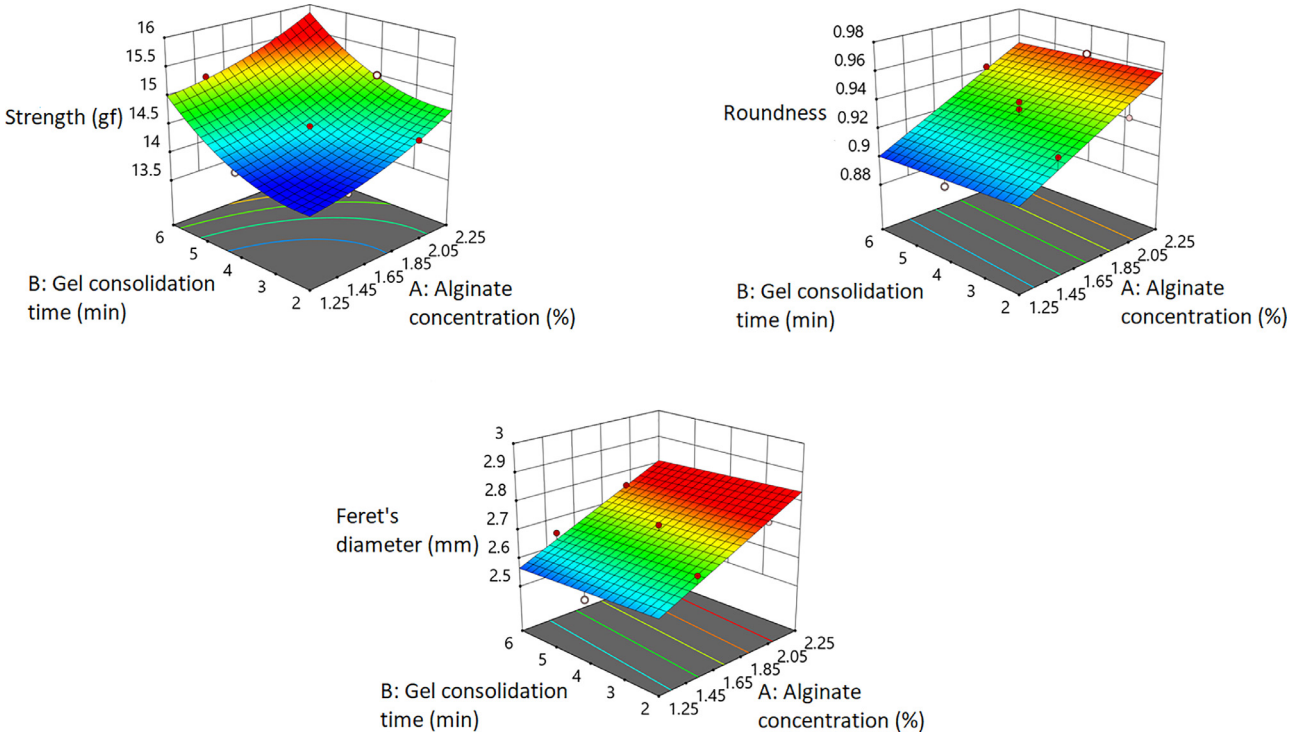

Fig. 2. RSM 3D surface for mechanical and morphological properties: **a)** Strength of beads, **b)** roundness, and **c)** Feret's diameter.

shown and further explained by microstructural parameters (Fig. 3). Rayment et al. (2009) found a direct correlation between the microstructure of the beads and their Young's modulus, obtaining higher values of strength for beads with denser internal structures. Jeong and coworkers (2020) also found that the strength required to rupture Ca(II)-alginate beads was directly proportional to alginate concentration under similar conditions to this study. For most industrial uses, beads should exhibit high values of strength which permits them to withstand shear stress during food processing. However, changes in microstructure, which in turn affect the strength, can have effects on the release of compounds in gastrointestinal conditions (Rayment et al., 2009). If beads were to be introduced as they are in ready-to-eat food, further

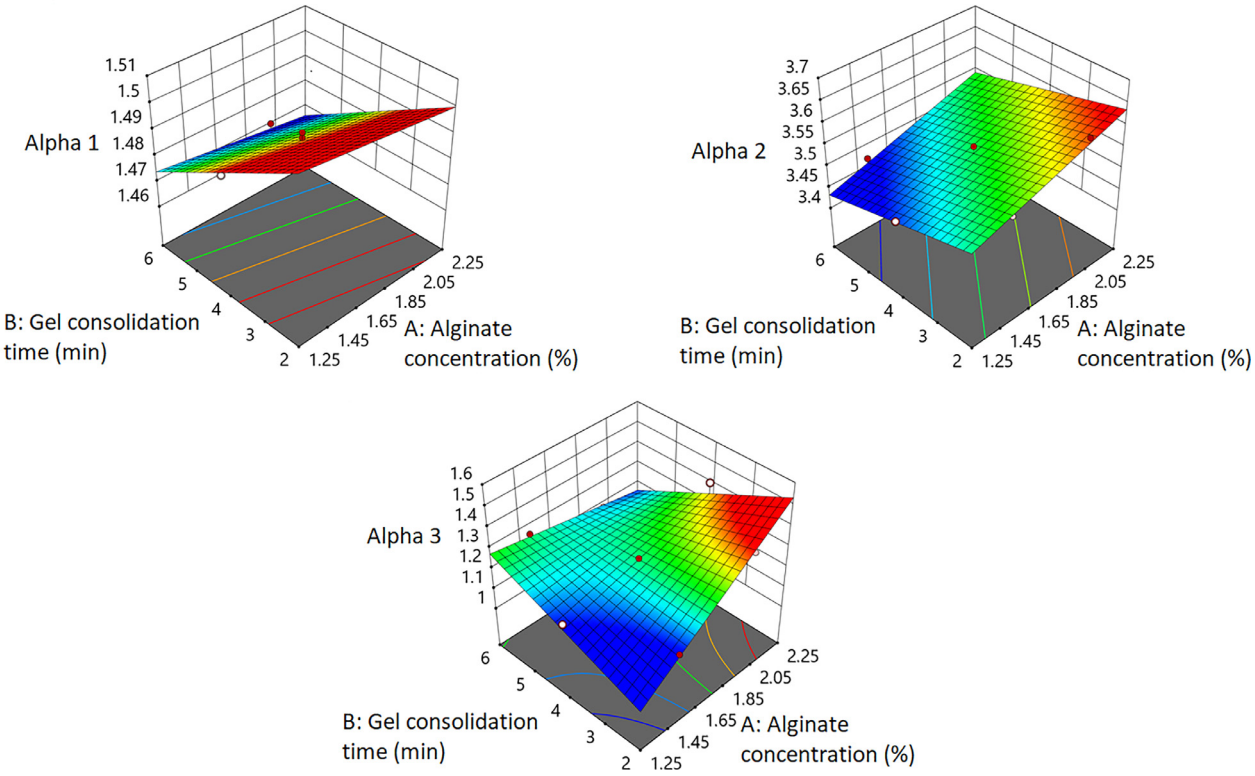

Fig. 3. RSM 3D surface for microstructural parameters: **a)** alpha 1, **b)** alpha 2 and **c)** alpha 3.

complementary sensory studies should be conducted as some food products could require stiffer and crunchier beads which broke easily while others could favor more chewy ones. Another important parameter that contributes to the mouthfeel of food is roundness which should be maximized to obtain beads as close as possible to perfect spheres. Studies demonstrate that shape is an influential factor in the perception of food, and it could also be associated to specific flavors and combinations of taste (Velasco et al., 2018). In this study, roundness was strongly dependent on alginate concentration, being directly proportional to it, while gel consolidation time did not have a significant effect (Table 1). Fig. S4 of the Supplementary File shows pictures of beads for each point in the RSM model. Zazzali and co-workers (2019) found no statistical differences in roundness for beads synthesized that had been allowed 5 minutes of hardening time with respect to beads that had remained in the gelling bath for days before being analyzed. Alginate concentration, on the other hand, has been linked to the roundness and sphericity of beads as it affects the viscosity of the dropping solution which determines the shape of the alginate droplet when impacting the gelling bath (Jeong et al., 2020). At lower alginate concentrations, or i.e., the viscosity of the dropping solution, the form of the alginate droplet may be easily reshaped when hitting the gelling bath, while increasing the alginate concentration could increment the surface tension thus maintaining a more spherical shape of the droplet without suffering many surface alterations. Finally, a similar trend was found between strength, roundness and Feret's diameter, especially in relation to their response to variations in alginate concentration. Considering these results and similar findings obtained by Zazzali et al. (2019) and Jeong et al., (2020), these phenomena could be subsumed under a broad category that is influenced and can be modulated by the concentration of the precursor.

When analyzing the modulation of microstructural parameters with alginate concentration and gel consolidation time, it is worth mentioning that all the hydrogels studied here, as a result of the concentrations of initial solutions and the short contact time of beads in the gelling bath, present a deficit in cross-linking cation with respect to the total guluronic sites available in the alginate polymer chains (i.e. the ratio Ca^{2+}:G-sites is under the stoichiometric relation). As reported in Posbeyikian et al., 2021, for similar Ca(II)-alginate systems, the complete gelation of the bead occurs in approximately 11 minutes in contact with the gelling bath. In these conditions, the initial process in the nucleation and growth of Ca(II)-alginate structures generates single "egg-box" structures, randomly dispersed in an interconnected structure, that can be modeled as rods with a higher fraction of free G-sites (Salvati, Santagapita, & Perullini, 2022). These unsaturated rods which still hold unlinked G-sites are expected to form a highly interconnected network due to the presence of abundant free branches of non-linked polymer. The fractal dimension of the alginate rods network which is related to the ramification of rods is represented with the α_1 parameter and its value depends on the ability of the incipient rods to interconnect with each other. With the synthesis conditions used in this work, the main contribution is observed for the variable of gel consolidation time, directly related to the availability of the crosslinker, Ca^{2+}, varying from 1.46-1.47 for the longest consolidation time explored (6 min), to 1.50-1.51 for the minimum consolidation time (2 min), as shown in Fig. 3-a. Reducing the gelling time hampers the cross-linking of alginate chains with Ca^{2+} ions and forms structures whereby free branches of unlinked polymer are favored, thus resulting in a more interconnected 3D network (higher values of α_1). Posbeyikian and co-workers (2021) described an analogous effect in the microstructure obtaining higher values of α_1 decreasing the ratio of Ca^{2+}:G-sites by increasing the concentrations of the alginate precursor from 2% to 3%. In this work alginate concentration only had a weak effect on α_1 (which is not statistically significant), similar to the conclusion found in Kuhn et al., (2021) for alginate concentrations between 1% and 1.25%, being time the predominant factor at these operational conditions. As mentioned above, in the time frame of our synthesis, time has a predominant role since the proportion of water in the core is greatly affected during the nascent stages of gel formation. However, especially at higher gelling times, a decrease in alginate concentration generates beads with lower strength and higher interconnec-

Table 2
Model and experimental values obtained for the validation of the experimental design. The graph for the desirability function is shown in Fig. **S5** of the Supplementary File.

Number	Alginate concentration (%)	Gel consolidation time (min)	TPC L.E (%)	RABTS (%)	RFRAP (%)	Strength (gf)	Roundness	α_1	Feret's diameter	Desirability
Model	2.25	2	39.50	24.30	24.96	14.75	0.96	1.50	2.84	0.95
Experimental			37.06	25.97	20.90	14.65	0.95	1.41	2.76	
Error %			**6.18**	**6.90**	**16.27**	**0.71**	**1.07**	**6.25**	**2.66**	

tivity. Zazzali et al. found in 2019 that beads generated at lower pH, i.e. with strong pre-existing alginate-alginate interactions, exhibited higher interconnectivity and lower strength. These findings suggest that conditions that favor strong preexisting interactions between alginate chains -due to hydrogen bonds- over Ca^{2+} crosslinking may lead to structurally weaker alginate gels.

The fractal dimension within the rods (α_2) is attributable to the degree of order in which dimers nucleate and aggregate during the formation of these primary structures. For this parameter, the concentration of the precursors (alginate polymer and Ca^{2+}, the latter being function of gelling time) has an important consequence in the kinetics of the process. In general terms, a higher concentration of precursors will generate a higher concentration of nucleation sites, where smaller and denser rods would result (higher values of parameter α_2). On the other hand, due to the strong electrostatic interaction between Ca^{2+} and G-sites, at a high concentration of divalent cations, the reordering of polymer branches to maximize weak interactions is hindered by a rapid crosslinking of the initial structure by Ca^{2+}. As predicted from this, in Fig. 3-b, the values of parameter α_2 increase from 3.42-3.47 to 3.54-3.63 with increasing alginate concentration, and show a slight decrease when increasing the time of consolidation in the $CaCl_2$ solution (i.e. increasing the availability of Ca^{2+} during the formation of rods and diminishing the possibility of rearrangement and densification of the rod structure).

At the smallest scale, parameter α_3 (shown in Fig. 3-c) denotes the fractal density of alginate dimers being a typical value $\alpha_3 \sim 1$. This value is generally obtained when the concentrations of both precursors (alginate and Ca^{2+}) are either high or low. A relative excess of one precursor, especially when alginate is in excess, is expected to lead to a more inhomogeneous arrangement of dimers and thus a higher value of α_3. As shown in Fig. 3-c, α_3 values are increased in zones of the RSM of maximum alginate concentration and minimum gel consolidation time and vice versa.

To the best of our knowledge, no works have been published on the encapsulation of phenolic compounds optimized for microstructural parameters. As we have shown, these parameters are significantly affected by the variation of some of the most important synthesis conditions and they are related to the studied physical and chemical properties. Hence, having a complete understanding of microstructural phenomena and being able to optimize for it in a Ca(II)-alginate encapsulation process allows for highly accurate and sophisticated tailoring necessary for precise delivery applications.

3.4. Optimal point and validation of the model

To identify the optimal experimental point, synthesis parameters were set to be in range with values used during this work, while TPC, ABTS AA, FRAP, strength, roundness and Feret's diameter were set to maximize due to their importance in potential applications of the beads. No goals were set for micro-structural parameters since as much correlation as they may have on the aforementioned responses; maximizing or minimizing them does not represent *per se* an improvement in the synthesis protocol for this particular work. However, α_1 was included in the optimization due to its significance regarding the microstructure of the gel and its discussed implications in the strength of beads. Table 2 shows experimental and model values for the best solution which corresponded to the maximum value of desirability (0.95). Other possible solutions for point predictions of the model are shown in Table S10 and Fig. S5 of the Supplementary File. The experimental encapsulation efficiency of TPC and residual antioxidant capacities obtained for the optimized beads synthesized during this work are in line with reports in the literature for Ca(II)-alginate beads without additives (Aguirre Calvo et al., 2018).

3.5. Phenolic compounds retention: from stem to Ca(II)-alginate

HPLC-MS analysis was performed on fresh artichoke sample, water extract according to the optimized procedure described by Zazzali et al. (2021) and freeze-dried alginate beads containing the water extract as reported in this work. This allowed us to evaluate the carryover of phenolic compounds from the initial sample to the alginate beads. These compounds boast many positive properties for human health including hypocholesterolemic, choleretic and antidyspeptic (Lattanzio et al., 2009). In a previous work (Zazzali et al., 2021) we performed a thorough analysis on phenolic compounds present in this variety of artichoke and found that isomers of the monocaffeoylquinic acid and dicaffeoylquinic acids were the most abundant phenolic compounds as has also been reported by several authors (Lattanzo et al., 2009; Mudau et al., 2018). In this work the monocaffeoylquinic and dicaffeoylquinic acids were the major phenolic compounds found. Mass spectra of monocaffeoylquinic acids showed the deprotonated molecule $[M - H]^-$ at m/z 353 and the MS^2 spectrum showed a peak at m/z 191 (quinic acid). Mass spectrum of dicaffeoylquinic acids showed the deprotonated molecule $[M - H]^-$ at m/z 515 and the MS^2 spectrum showed peaks at m/z 353, 191 and 179 which are typical of dicaffeoylquinic acids (Abu-Reidah et al., 2013). Our results showed that 3-caffeoylquinic acid, 5-caffeoylquinic acid, and two isomers of a dicaffeoylquinic acid, which account for most of the bioactive properties of the artichoke, are present in all samples thus confirming that preservation was achieved during the water extraction and further encapsulation process. Chromatographic and MS data of phenolic compounds from raw artichoke, water extract and encapsulated water extract are shown in **Table S11-S13** of the Supplementary File.

4. Conclusions

To achieve sustainability and SDG, it is mandatory to consider several points of view. From a technological perspective, the complete valorization of a waste includes not only its fundamental chemistry, but also the means to its inclusion in apliccations with a versatile technology. The present work deals with ~~to~~ the optimization of a cheap and scalable encapsulation technology that can be used in pharmaceutical, nutraceutical and food industries. Satisfactory models have been presented for the optimization of a Ca(II)-alginate encapsulation of bioactive compounds from artichoke waste, achieving the maximum values of bioactive properties (TPC, RSA and RFRAP) as well as mechanical and morphological parameters (strength and roundness of beads). In addition, the most abundant and important phenolic compounds are successfully carried over from the artichoke waste to the encapsulated extract. While higher values of bioactive properties and roundness are almost always desirable, the strength of the beads should be evaluated

on a case-by-case basis according to the application of the beads and possibly complemented by sensory studies for nutraceutical and food uses. The model was also optimized for microstructural parameters and microstructural phenomena was explained as a function of precursor concentration and gelation time. Given these considerations, studying the α_1 parameter could be useful to predict and modulate the strength behavior of beads from a microstructural standpoint by varying the concentration of the precursor solutions and synthesis parameters related to their availability. This profound understanding of the internal structure of the gel matrix could allow for state-of-the-art optimization and modulation of the fine structure in advanced applications.

Ethical Statement – Studies in humans and animals

The authors declare that this work does not involve the use of human subjects or human data. Additionally, the authors declare that no animal experiments were carried out.

Declaration of Competing Interests

The authors declare that they have no known competing financial interests or personal relationships that could have appeared to influence the work reported in this paper.

Data Availability

Data will be made available on request.

Acknowledgments

This work was supported by the Brazilian Synchrotron Light Laboratory (LNLS, Brazil, proposals SAXS1-20190143 and SAXS1-20190073), Agencia Nacional de Promoción Científica y Tecnológica (ANPCyT PICT-2017-0569 and PICT-2020-3745), and Consejo Nacional de Investigaciones Científicas y Técnicas (IZ PhD scholarship).

Supplementary materials

Supplementary material associated with this article can be found, in the online version, at doi:10.1016/j.fhfh.2022.100097.

References

Abu-Reidah, IM, Arráez-Román, D, Segura-Carretero, A, & Fernández-Gutiérrez, A (2013). Extensive characterisation of bioactive phenolic constituents from globe artichoke (*Cynara scolymus* L.) by HPLC-DAD-ESI-QTOF-MS. *Food Chemistry, 141*(3), 2269–2277.

Aguirre Calvo, TR, Perullini, M, & Santagapita, PR (2018). Encapsulation of betacyanins and polyphenols extracted from leaves and stems of beetroot in Ca(II)-alginate beads: A structural study. *Journal of Food Engineering, 235*, 32–40.

Aguirre Calvo, TR, Molino, S, Perullini, M, Rufián-Henares, JA, & Santagapita, PR (2020). Effect of *in vitro* digestion-fermentation of Ca(II)-alginate beads containing sugar and biopolymers over global antioxidant response and short chain fatty acids production. *Food Chemistry, 333*, 127483–127492.

Agulhon, P, Robitzer, M, Laurent, D, & Quignard, F (2012). Structural regime identification in ionotropic alginate gels: Influence of the cation nature and alginate structure. *Biomacromolecules, 13*(1), 215–220.

Astley, S, & Finglas, P (2016). Nutrition and health. *Reference Module in Food Science*.

Benzie, IF, & Strain, JJ (1996). The ferric reducing ability of plasma (FRAP) as a measure of "antioxidant power": The FRAP assay. *Analytical Biochemistry, 239*, 70–76.

He, X, Liu, Y, & Li, H (2016). Single-stranded structure of alginate and its conformation evolvement after an interaction with calcium ions as revealed by electron microscopy. *RSC Advances, 6*(115), 114779–114782.

Jeong, C, Kim, S, Lee, C, Cho, S, & Kim, S (2020). Changes in the physical properties of calcium alginate beads under a wide range of gelation temperature conditions. *Foods, 9*, 180.

King, AH (1983). Brown seaweed extracts (Alginates). In M. Glicksman (Ed.), *Food Hydrocolloids* (pp. 115–188). Boca Raton Florida: CRC Press.

Kuhn, F, Santagapita, PR, & Zapata Noreña, CP (2021). Influence of egg albumin and whey protein in the co-encapsulation of betalains and phenolic compounds from *Bougainvillea glabra* bracts in Ca(II)-alginate beads. *Journal of Food Processing and Preservation, 45*, e15918.

Lattanzio, V, Kroon, PA, Linsalata, V, & Cardinali, A (2009). Globe artichoke: A functional food and source of nutraceutical ingredients. *Journal of Functional Foods, 1*(2), 131–144.

Madalena, DA, Pereira, RN, Vicente, A,A, & Ramos, OL (2019). New insights on bio-based micro- and nanosystems in food. *Encyclopediaa of Food Chemistry*, 708–714.

Mudau, SP, Steenkamp, PA, Piater, LA, De Palma, M, Tucci, M, Madala, NE, & Dubery, IA (2018). Metabolomics-guided investigations of unintended effects of the expression of the *hydroxycinnamoyl quinate hydroxycinnamoyltransferase* (*hqt*1) gene from *Cynara cardunculus* var. *scolymus* in *Micotiana tabacum* cell cultures. *Plant Physiology and Biochemistry, 127*, 287–298.

Narayanan, RP, Melman, G, Letourneau, NJ, Mendelson, NL, & Melman, A (2012). Photodegradable iron (III) cross-linked alginate gels. *Biomacromolecules, 13*, 2465–2471.

Perullini, M, Ferro, Y, Durrieu, D, Jobagy, M, & Bilmes, SA (2014). Sol-gel silica platforms for microalgae-based optical biosensors. *Journal of Biotechnology, 179*, 65–70.

Posbeyikian, A, Tubert, E, Bacigalupe, A, Escobar, MM, Santagapita, PR, Amodeo, G, & Perullini, M (2021). Evaluation of calcium alginate bead formation kinetics: An integrated analysis through light microscopy, rheology and microstructural SAXS. *Carbohydrate Polymers, 269*, 118293.

Rayment, P, Wright, P, Hoad, C, Ciampi, E, Haydock, D, & Gowland, P (2009). Investigation of alginate beads for gastrointestinal functionality, part 1: In vitro characterization. *Food Hydrocolloids, 23*, 816–822.

Re, R, Pellegrini, N, Proteggente, A, Pannala, A, Yang, M, & Rice-Evans, C (1999). Antioxidant activity applying an improved ABTS radical cation decolorization assay. *Free Radical & Biological Medicine, 26*, 1231–1237.

Rodrigues, E, Mariutti, LRB, & Mercadante, AZ (2013). Carotenoids and phenolic compouns from *Solanum sessiliflorum*, an unexploited amazonian fruit, and their scavenging capacities against reactive oxygen and nitrogen species. *Journal of Agricultural and Food Chemistry, 61*, 3022–3029.

Salvati, B, Santagapita, P, & Perullini, M (2022). Exploring the conditions to generate alginate nanogels. *Journal of Sol-Gel Science and Technology, 102*, 142–150.

Santos, D,I, Saraiva, JMA, Vicente, AA, & Moldao-Martins, M (2019). Methods for determining bioavailability and bioaccessibility of bioactive compounds and nutrients. *Innovative Thermal and Non-Thermal Processing, Bioaccessibility and Bioavailability of Nutrients and Bioactive Compounds*, 23–54.

Serrano, JCE, Cassanye, A, Martín-Gari, M, Granado-Serrano, A,B, & Portero-Otín, M (2016). Effect of dietary bioactive compounds on mitochondrial and metabolic flexibility. *Diseases, 4*, 14 2016.

Singleton, VL, & Lamuela-Raventós, RM (1999). Analysis of total phenols and other oxidation substrates and antioxidants by means of Folin-Ciocalteu reagent. *Methods in Enzymology, 299*, 152–178.

Sonego, JM, Santagapita, PR, Perullini, M, & Jobbágy, M (2016). Ca(II) and Ce(III) homogeneous alginate hydrogels from the parent alginic acid precursor: A structural study. *Dalton Transactions, 45*(24), 10050–10057.

Spence, C, & Ngo, MK (2012). Assessing the shape of symbolism of the taste, flavor, and texture of foods and beverages. *Flavour, 1*(2).

Stokke, BT, Draget, KI, Smidsrod, O, Yuguchi, Y, Urakawa, H, & Kajiwara, K (2000). Small-angle X-ray scattering and rheological characterization of alginate gels. 1. Ca-alginate gels. *Macromolecules, 33*(5), 1853–1863.

Traffano-Schiffo, MV, Castro-Giraldez, M, Fito, PJ, Perullini, M, & Santagapita, PR (2018). Gums induced microstructure stability in Ca(II)-alginate beads containing lactase analyzed by SAXS. *Carbohydrate Polymers, 179*, 402–407.

Tungmunnithum, D, Thongboonyou, A, Pholboon, A, & Yangsabai, A (2018). Flavonoids and other phenolic compounds from medicinal plants for pharmaceutical and medical aspects: An overview. *Medicines, 5*(3), 93.

Velasco, C, Obrist, M, Petit, O, & Spence, C (2018). Multisensory technology for flavor augmentation: A mini review. *Frontiers in Psychology, 9*, 26.

Zazzali, I, Aguirre Calvo, TR, Pizones Ruíz-Henestrosa, VM, Santagapita, PR, & Perullini, M (2019). Effects of pH, extrtusion tip size and storage protocol on the structural properties of Ca(II)-alginate beads. *Carbohydrate Polymers, 206*, 749–756.

Zazzali, I, Gabilondo, J, Peixoto Mallmann, L, Rodrigues, E, Perullini, M, & Santagapita, PR (2021). Overall evaluation of artichoke leftovers: Agricultural measurement and bioactive properties assessed after green and low-cost extraction methods. *Food Bioscience, 41*, 100963.